


The long non-coding RNA LINC00941 and SPRR5 are novel regulators of human epidermal homeostasis

Christian Ziegler^{1,†}, Johannes Graf^{1,†}, Stefan Faderl¹, Jessica Schedlbauer¹, Nicholas Strieder², Bianca Förstl¹, Rainer Spang², Astrid Bruckmann¹, Rainer Merkl³, Sonja Hombach¹ & Markus Kretz^{1,*} 

Abstract

Several long non-coding RNAs (lncRNAs) act as regulators of cellular homeostasis; however, few of these molecules were functionally characterized in a mature human tissue environment. Here, we report that the lncRNA LINC00941 is a crucial regulator of human epidermal homeostasis. LINC00941 is enriched in progenitor keratinocytes and acts as a repressor of keratinocyte differentiation. Furthermore, LINC00941 represses SPRR5, a previously uncharacterized molecule, which functions as an essential positive regulator of keratinocyte differentiation. Interestingly, 54.8% of genes repressed in SPRR5-deficient epidermal tissue are induced in LINC00941-depleted organotypic epidermis, suggesting a common mode of action for both molecules.

Keywords differentiation; epidermis; LINC00941; long non-coding RNA; SPRR5

Subject Categories Development & Differentiation; RNA Biology

DOI 10.15252/embr.201846612 | Received 19 June 2018 | Revised 29 November 2018 | Accepted 4 December 2018 | Published online 8 January 2019

EMBO Reports (2019) 20: e46612

Introduction

The epidermis is a stratified surface epithelium that provides a protective barrier to the external environment and constantly self-renews approximately every 28 days. During this regeneration process, progenitor cells settled in the basal layer divide and the daughter cells undergo a terminal differentiation program. A precise balance between keratinocytes in the progenitor compartment and terminally differentiated layers is crucial to ensure formation of a functional epidermis with an intact water barrier [1]. Disrupted expression of genes controlling proliferation and differentiation occurs in numerous skin diseases and epidermal cancers [2]. Thus, further understanding of these processes will give insight into normal tissue homeostasis

and may provide new targets for the prevention and treatment of disorders of epidermal growth, differentiation, and regeneration.

Long non-coding RNAs (lncRNAs) have emerged as key regulators of gene expression in many different cellular pathways and were frequently shown to act as part of protein-containing complexes [3]. Nevertheless, the exact genomic annotations and functional significance for most lncRNAs are still unknown to date. Few lncRNAs were shown to be functionally involved in normal human epidermal homeostasis: ANCR, TINCR, and SMRT-2 appear to regulate differentiation, while PRINS is a stress-regulated lncRNA involved in psoriasis [4–9]. However, the majority of functionally characterized lncRNAs regulate developmental processes and their potential role in controlling mature tissue homeostasis and differentiation remains largely uncharacterized.

Here, we show that the long non-coding RNA LINC00941 functions as a crucial regulator of human epidermal homeostasis. LINC00941 is enriched in progenitor keratinocytes and acts as a repressor of keratinocyte differentiation in cells and tissue. LINC00941 represses SPRR5, a previously uncharacterized predicted protein, which we show functions as an essential regulator of keratinocyte differentiation. SPRR5 is located within the epidermal differentiation complex (EDC) and controls expression of the small proline-rich region (SPRR) and late cornified envelope (LCE) differentiation gene clusters. Thus, LINC00941 appears to inhibit premature differentiation in weakly differentiated strata of the human epidermis, at least in part, through repression of SPRR5.

Results and Discussion

The long non-coding RNA LINC00941 is enriched in human progenitor keratinocytes

To identify previously unrecognized lncRNAs involved in human epidermal homeostasis, we recently conducted transcriptome sequencing analyses of non-differentiated and differentiated human

¹ Institute of Biochemistry, Genetics and Microbiology, University of Regensburg, Regensburg, Germany

² Statistical Bioinformatics Department, Institute of Functional Genomics, University of Regensburg, Regensburg, Germany

³ Institute of Biophysics and Physical Biochemistry, University of Regensburg, Regensburg, Germany

*Corresponding author. Tel: +49 941 9431748; E-mail: Markus.Kretz@ur.de

[†]These authors contributed equally to this work

keratinocytes and revealed a number of lncRNAs dynamically regulated throughout this process [5,6]. One of these lncRNAs, LINC00941, which is encoded on chromosome 12, was most highly expressed in undifferentiated progenitor keratinocytes (on average approximately 59 ± 14 copies per cell) and significantly reduced in abundance upon onset of terminal differentiation. Correspondingly, qRT-PCR analysis confirmed reduction of LINC00941 expression throughout all time points of calcium-induced differentiation of human keratinocyte cultures (Fig 1A). While LINC00941 was recently reported to play a role in development of hepatocellular carcinoma [10], nothing is known about its role in regulation of tissue homeostasis. LINC00941 is expressed in multiple human tissues

(Fig EV1A) and annotated as a lncRNA with two isoforms with a length of 1,895 and 1,355 nucleotides, respectively (Fig EV1B).

To verify the annotation of LINC00941 as a long non-coding RNA, we utilized Coding-Potential Assessment Tool (CPAT [11], iSeeRNA [12], Lncident [13], and Coding Potential Calculator CPC2 [14]) to assess the coding potential of the nucleotide sequences (Fig EV1C). We could confirm lack of protein-coding potential with either of the algorithms used, strongly indicating that LINC00941 solely acts as a long non-coding RNA (Fig EV1C). Cellular fractionation of undifferentiated human keratinocytes indicated presence of LINC00941 in both cytoplasmic and nuclear compartments, with an increased nuclear enrichment compared to mRNAs (Fig EV1D). To

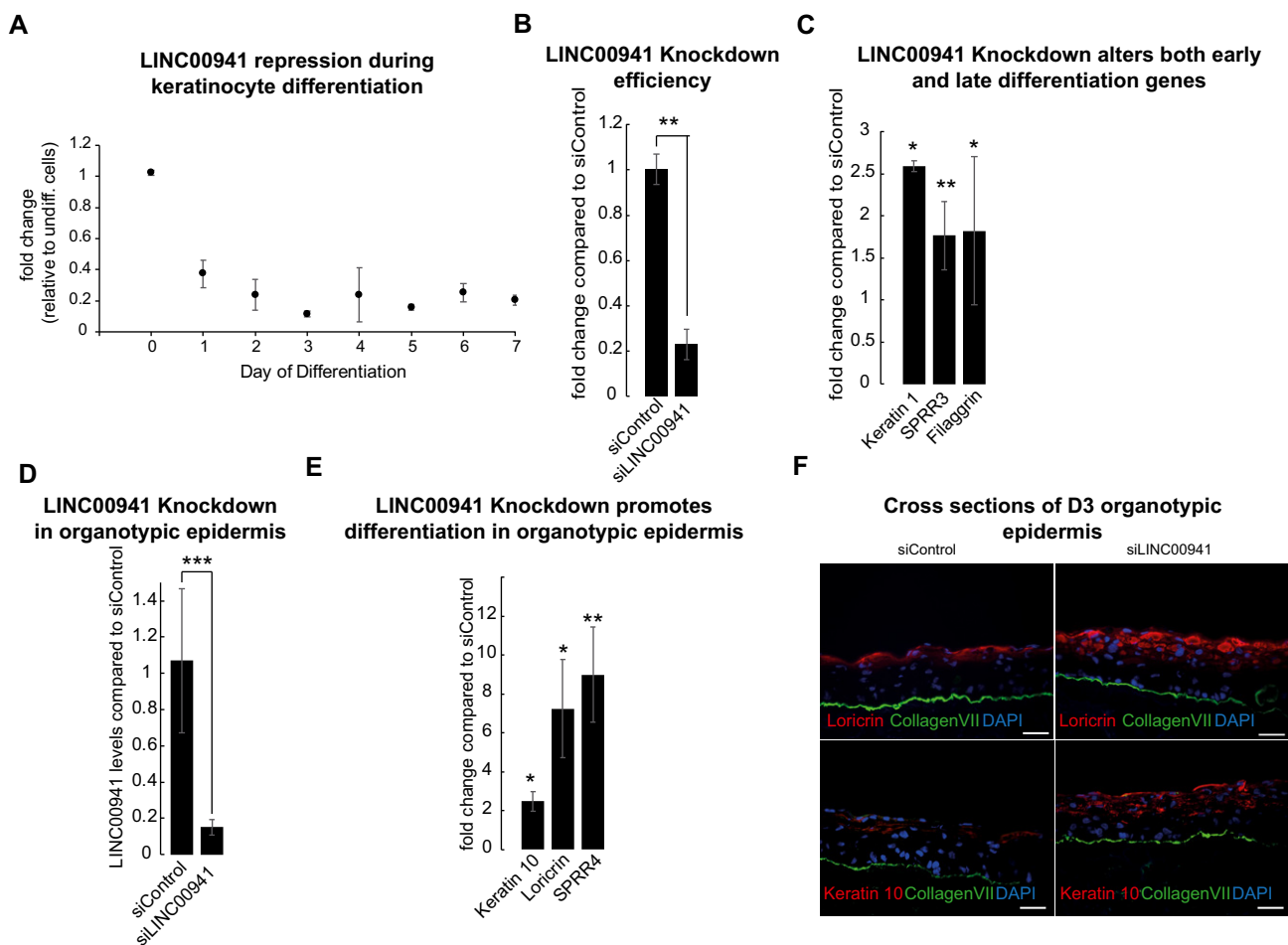


Figure 1. LINC00941 acts as a negative regulator of keratinocyte differentiation.

- A qRT-PCR analysis of LINC00941 repression during keratinocyte differentiation in primary keratinocyte cultures from three different donors compared to undifferentiated keratinocytes (D0) ($n = 6$ biological replicates). Data are presented as mean \pm SD.
- B, C siPool-mediated LINC00941 knockdown (B) in calcium-induced keratinocyte differentiation results in increased abundance of early and late differentiation marker transcripts on day 3 of differentiation (C) ($n = 3$ biological replicates/knockdown group). Data are presented as mean \pm SD. Statistical significance was tested by an unpaired *t*-test and corrected for multiple testing after Bonferroni (*adj. *P*-value < 0.05, **adj. *P*-value < 0.01).
- D, E LINC00941 knockdown in day 3 (D3) organotypic epidermal tissue cultures (D) results in increased expression of key differentiation genes (E) ($n = 3$ –4 tissue cultures/knockdown group). Data are presented as mean \pm SD. Statistical significance was tested by an unpaired *t*-test and corrected for multiple testing after Bonferroni (*adj. *P*-value < 0.05, **adj. *P*-value < 0.01, ***adj. *P*-value < 0.001).
- F Immunofluorescence analysis shows increased levels of early and late differentiation proteins. Collagen VII (col VII, green) stain indicates the basement membrane, nuclei are shown in blue, and the differentiation proteins keratin 10 and loricrin are shown in red ($n = 3$ –4 tissue cultures/knockdown group; one exemplary picture for each group is depicted). Scale bar: 50 μ m.

assess LINC00941 localization in epidermal tissue, we measured LINC00941 abundance at different time points of organotypic epidermal tissue regeneration. In agreement with LINC00941 dynamic regulation during keratinocyte differentiation, we observed highest LINC00941 abundance at day zero of epidermis development (Fig EV1E).

LINC00941 prevents premature differentiation of human keratinocytes

Since LINC00941 abundance decreases upon keratinocyte differentiation, we postulated a role for this lncRNA in non- or poorly differentiated strata of the epidermis. To test this hypothesis, we generated LINC00941-deficient keratinocytes by transfection of a pool of 30 siRNAs and found that loss of LINC00941 resulted in an increased abundance of mRNA levels for early and late differentiation genes, suggesting a functional relevance of LINC00941 in preventing premature progression of the terminal differentiation program (Fig 1B and C).

To analyze the impact of LINC00941 on the homeostatic balance of human epidermal tissue, we generated LINC00941-deficient human organotypic epidermis and compared it with matching control tissue (Fig 1D). Similar to results observed with primary keratinocytes, LINC00941-deficient organotypic epidermis differentiated prematurely, as indicated by increased mRNA and protein abundances of keratin 10, crucial for early differentiation, as well as late differentiation genes *SPRR4* and *Loricrin* (Fig 1E and F). These results indicate an important role for LINC00941 in repressing premature keratinocyte differentiation in cells and human epidermal tissue.

LINC00941 regulates transcript abundance of early and late differentiation genes

To probe the global impact of LINC00941 deficiency on gene expression during human epidermal homeostasis, we performed whole transcriptome sequencing analysis of LINC00941-depleted as well as control organotypic epidermis (Fig 2A and B) at days 2 and 3 after onset of epidermal homeostasis and identified 240 and 314 genes, respectively, that were deregulated upon LINC00941 loss (Figs 2C and EV2A–C, Dataset EV1A and B). Gene ontology (GO) term analysis of deregulated genes in LINC00941-deficient tissue showed strong enrichment of genes involved in processes crucial for epidermal differentiation, such as keratinization, keratinocyte differentiation, generation of a cornified envelope, and peptide cross-linking (Figs 2D and EV2B). These findings provide further evidence for a role of LINC00941 in repressing the epidermal differentiation program. To investigate potential hot spots of LINC00941-regulated genes across the human genome, we analyzed enrichment of LINC00941-altered genes compared to the relative distribution of Ensembl genes across all human chromosomes. The strongest enrichment could be detected on chromosome one (Fig EV2D), with a significant accumulation of altered genes in the epidermal differentiation complex (1q21.3; EDC; Fig 3A). The EDC spans 1.9 Mb and harbors roughly sixty genes, many of which coding for proteins involved in keratinocyte differentiation and epidermal barrier formation [15,16]. Correspondingly, 28 well-characterized genes crucial for epidermal differentiation located within the EDC show

premature expression in LINC00941-depleted epidermal tissue (Fig 2C). These include *Loricrin*, *SPRR4*, and 16 out of 18 *LCE* genes. Thus, LINC00941 is capable of repressing key differentiation genes and preventing premature onset of differentiation in human epidermal tissue.

SPRR5 is a LINC00941- and p63-regulated uncharacterized gene induced in keratinocyte differentiation

In addition to well-characterized early and late differentiation genes, LINC00941 deficiency led to induced expression of an uncharacterized gene locus comprising the long non-coding RNA LINC01527, as well as the recently annotated *SPRR5* transcript, which is located within the EDC, 35-kb downstream of *Involucrin* and 21-kb upstream of the small proline-rich protein gene cluster (Fig EV3A). Interestingly, a significant induction of *SPRR5* (but not LINC01527) could be detected in all biological replicates used in the transcriptome sequencing analysis and was confirmed in qRT-PCR analysis of LINC00941 deficient vs. control tissue (Fig 3B and C).

Employing northern blot as well as qRT-PCR analysis, we found *SPRR5* expression to be barely detectable in non-differentiated, primary human keratinocytes. Upon onset of epidermal differentiation however, *SPRR5* abundance was strongly increased, with the highest levels at late differentiation stages (Fig 3D and E). For in-depth characterization of the *SPRR5* gene locus, we performed a combination of northern blot mapping and rapid amplification of cDNA ends (RACE) analysis and found that the *SPRR5* transcript in human primary keratinocytes does not match the recent Ensembl annotation. Instead, we could verify a shorter transcript with a length of 762 nucleotides, consisting of two exons (Figs EV3B and EV4A). The annotated lncRNA LINC01527, located in antisense direction to *SPRR5*, showed no detectable expression with all detection methods employed in this study. In order to identify additional regulators of *SPRR5* expression, computational predictions of upstream transcription factors for *SPRR5* were performed. We observed strong enrichment of p63 (Fig EV3C), a transcription factor known to act as a master regulator of human and mouse epidermal homeostasis [17–19]. p63 is well known to act as an important regulator of epidermal commitment, keratinocyte proliferation, and also of differentiation [19–22]. Correspondingly, ChIP sequencing analyses published recently [20,21] indicated sites of p63 occupancy 5 kb upstream and 4 kb downstream of the *SPRR5* gene locus (Fig EV3D). To test whether *SPRR5* expression might indeed be regulated by p63, we knocked down p63 in differentiated human keratinocytes and observed a strong reduction of *SPRR5* transcript abundance by 91%. Interestingly, knockdown of p63 did not significantly affect abundance of LINC00941, suggesting that LINC00941 is transcriptionally regulated independently of p63 (Fig 3F). Additionally, knockdown of LINC00941 in human epidermal tissue does not affect p63 (Fig EV3E). Together, these findings show that *SPRR5* is controlled by the transcription factor p63 and prematurely induced in LINC00941-deficient human organotypic epidermis.

SPRR5 is essential for human epidermal differentiation

To analyze a potential functional impact of *SPRR5* on epidermal differentiation, we depleted *SPRR5* in human keratinocytes with a

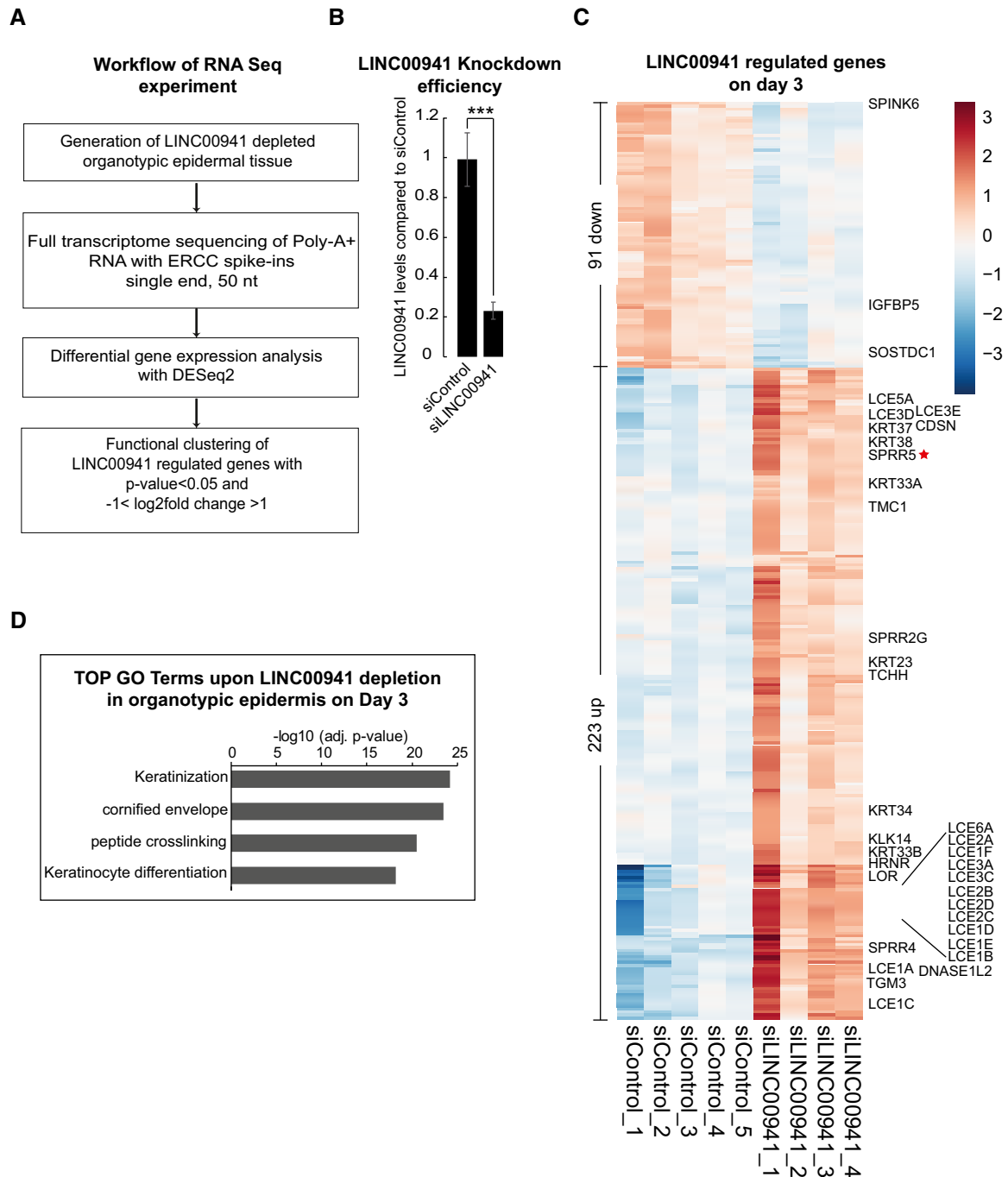


Figure 2. LINC00941 is a suppressor of keratinocyte differentiation.

- A Workflow of the performed RNA-sequencing experiment.
- B LINC00941 knockdown efficiency (siLINC00941) in epidermal tissue on day 3 of differentiation as obtained by qRT-PCR measurements ($n = 4\text{--}5$ epidermal tissue cultures/knockdown group). Data are presented as mean \pm SD. Statistical significance was tested by an unpaired t -test and corrected for multiple testing after Bonferroni (***)adj. P -value < 0.001).
- C Heatmap of differentially expressed genes ($P_{\text{adj}} < 0.05$ and $-1 > \log_2\text{FC} > 1$) upon LINC00941 depletion on day 3 in organotypic epidermal tissue with marked keratinocyte differentiation genes ($n = 4\text{--}5$ epidermal tissue cultures/knockdown group).
- D GO term analysis of downregulated ($P_{\text{adj}} < 0.05$ and $-1 > \log_2\text{FC} < 1$) genes in LINC00941-deficient organotypic epidermal tissue on day 3 ($n = 4\text{--}5$ epidermal tissue cultures/knockdown group).

siRNA pool and measured mRNA and protein abundances of key differentiation genes at days 4, 5, and 6 of keratinocyte differentiation using qRT-PCR and Western blot analysis. Interestingly, SPRR5

deficiency led to a decreased expression of early and late differentiation genes during all time points analyzed (Fig 4A–C). In order to verify the observed functional impact of SPRR5 in a mature human

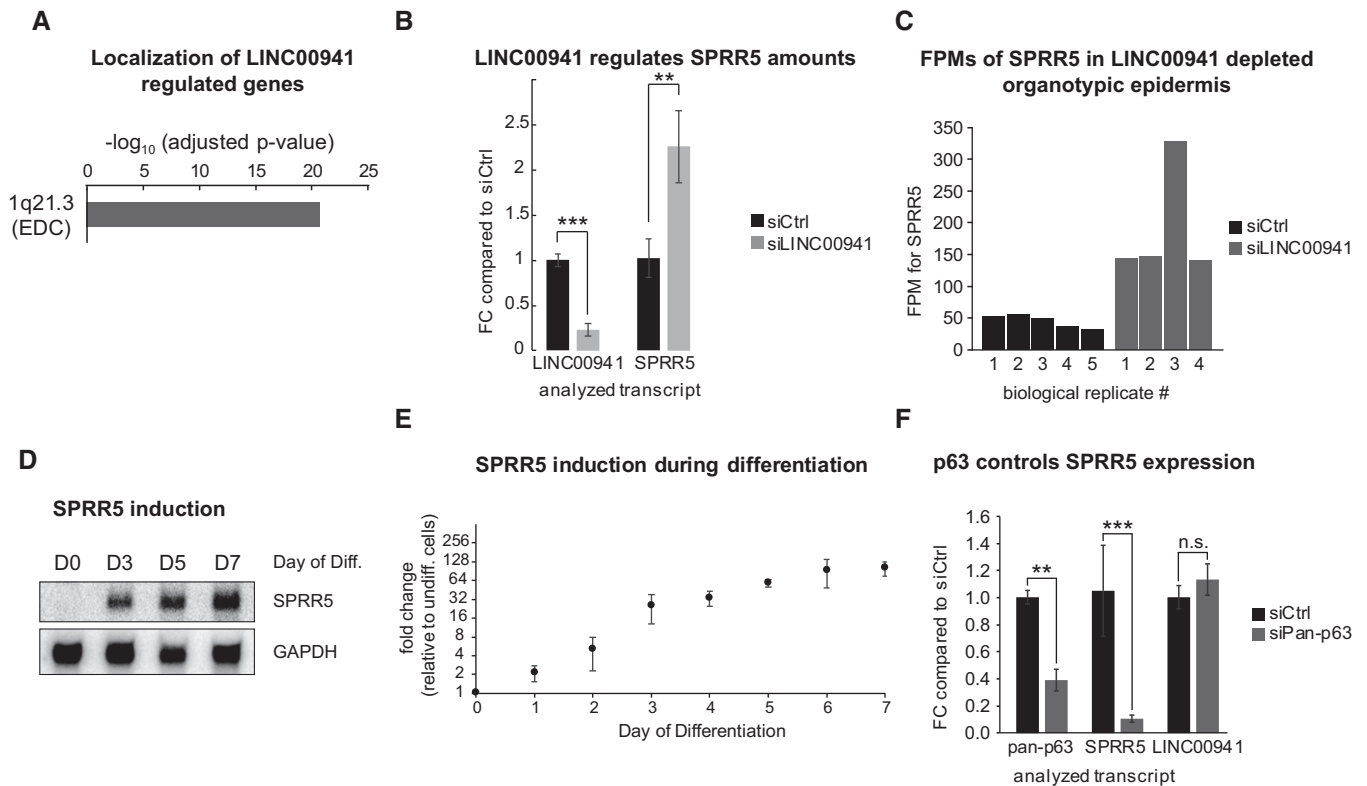


Figure 3. LINC00941 and p63 control SPRR5, which is induced during differentiation and different from other human SPRRs.

- A Differentially expressed genes in day 3 LINC00941-depleted epidermal tissue cluster within the epidermal differentiation complex (EDC) ($n = 4\text{--}5$ biological replicates/knockdown group).
- B LINC00941 knockdown on day 3 in calcium-induced keratinocyte differentiation cultures results in increased expression of SPRR5 (FC = fold change; $n = 3$ biological replicates/knockdown group). Data are presented as mean \pm SD. Statistical significance was tested by an unpaired *t*-test and corrected for multiple testing after Bonferroni (**adj. *P*-value < 0.01 , ***adj. *P*-value < 0.001).
- C Detected fragments per million (FPM) for SPRR5 in control (siCtrl) as well as LINC00941-deficient (siLINC00941) epidermal tissue for all biological replicates on day 3 (D3) of differentiation as obtained by DeSeq2 (FC = fold change; $n = 4\text{--}5$ epidermal tissue cultures/knockdown group).
- D, E SPRR5 induction during the course of keratinocyte (KC) differentiation is shown by northern blot (D) as well as by qRT-PCR analysis (E) for four different primary keratinocyte isolates and compared to undifferentiated keratinocytes ($n = 8$ biological replicates). Data are presented as mean \pm SD.
- F p63 knockdown on day 3 of keratinocyte differentiation leads to decreased SPRR5 transcript levels (FC = fold change; $n = 3\text{--}4$ biological replicates/knockdown group). Data are presented as mean \pm SD. Statistical significance was tested by an unpaired *t*-test and corrected for multiple testing after Bonferroni (*adj. *P*-value < 0.05 , **adj. *P*-value < 0.01 , ***adj. *P*-value < 0.001 , and n.s. = not significant).

tissue environment, we generated SPRR5-deficient human organotypic epidermis. Similar to results seen with primary keratinocytes, SPRR5-deficient epidermal tissue displays defective differentiation as seen by reduced levels of a plethora of early and late differentiation mRNAs and proteins (Fig 4D–F).

For a more comprehensive insight on the functional impact of this previously uncharacterized molecule on epidermal homeostasis, we performed full transcriptome sequencing with RNA isolated from SPRR5-deficient and control organotypic epidermis at two different time points of tissue growth (Fig 5A and B). SPRR5 depletion resulted in abnormal abundance of 249 and 379 transcripts at days 3 and 4 of epidermal regeneration, respectively (Figs 5C and D, and EV4B and C, Dataset EV1C and D). Furthermore, the top five gene ontology terms of transcripts downregulated in SPRR5-deficient tissue were keratinocyte differentiation, keratinization, cornified envelope, epidermis development, and peptide cross-linking—all representing key processes of terminal differentiation (Fig 5E

and F). As we mapped all SPRR5-regulated genes to the human genome, we observed a strong enrichment within the EDC where over 50% of genes exhibited altered expression after SPRR5 depletion. In summary, these data suggest a crucial role for SPRR5 in regulating and maintaining the terminal differentiation program in human epidermal tissue by inducing genes strongly associated with epidermal differentiation, many of which are located within the EDC.

LINC00941 prevents premature differentiation partially through inhibition of SPRR5

Our findings indicate that LINC00941 represses premature differentiation in weakly differentiated strata, while SPRR5 promotes terminal differentiation of human epidermal tissue. To investigate whether the lncRNA LINC00941 and SPRR5 conversely regulate a common set of genes, we analyzed the overlap between transcripts induced

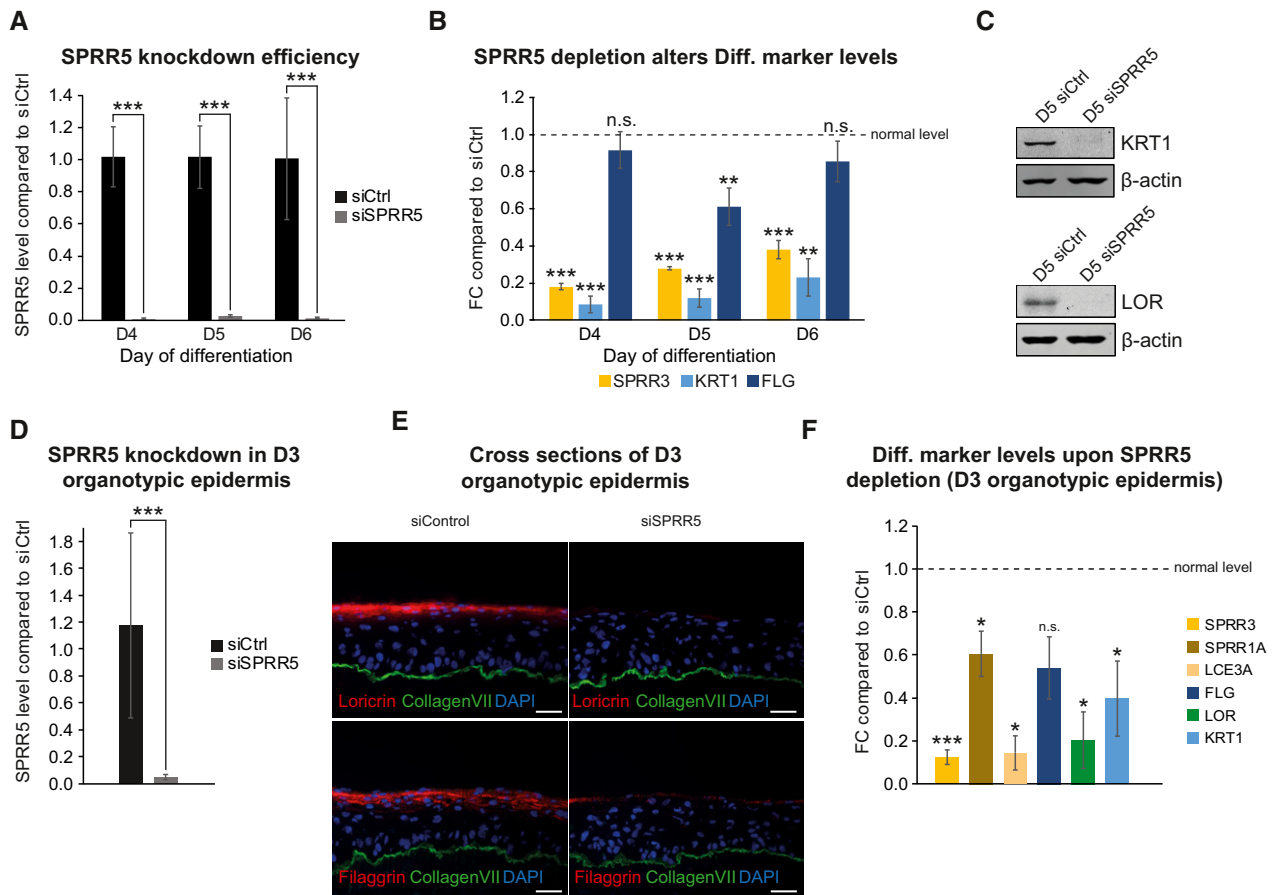


Figure 4. SPRR5 is indispensable for proper keratinocyte differentiation.

A–C siPool-mediated SPRR5 knockdown on day 4 to day 6 (D4–D6) of calcium-induced keratinocyte differentiation (A) leads to decreased expression of key differentiation markers as shown by qRT–PCR (B) (FC = fold change) as well as Western blot analysis (C) ($n = 3–5$ cultures/knockdown group). Data are presented as mean \pm SD. Statistical significance was tested by an unpaired t -test and corrected for multiple testing after Bonferroni (**adj. P -value < 0.01, ***adj. P -value < 0.001, and n.s. = not significant).

D SPRR5 knockdown efficiency in day 3 (D3) organotypic epidermal tissue ($n = 4$ epidermal tissue cultures/knockdown group). Data are presented as mean \pm SD. Statistical significance was tested by an unpaired t -test and corrected for multiple testing after Bonferroni (**adj. P -value < 0.001).

E SPRR5 depletion in regenerated organotypic epidermal tissue results in drastically reduced expression of differentiation proteins as shown by immunofluorescence analysis. Collagen VII (Col VII, green) stain indicates the basement membrane, nuclei are shown in blue, and the differentiation proteins filaggrin and loricrin are shown in red ($n = 4$ tissue cultures/knockdown group; one exemplary picture for each group is depicted). Scale bar: 50 μ m.

F SPRR5 knockdown in regenerated epidermal tissue results in reduced transcript levels of key differentiation genes as obtained by qRT–PCR ($n = 4$ epidermal tissue cultures/knockdown group). Data are presented as mean \pm SD. Statistical significance was tested by an unpaired t -test and corrected for multiple testing after Bonferroni (*adj. P -value < 0.05, ***adj. P -value < 0.001, and n.s. = not significant).

upon LINC00941 depletion (223 in total) and mRNAs down-regulated in SPRR5-deficient tissue (Fig 5G and Dataset EV1E). Interestingly, 54.8% (69 from a total of 126) of genes repressed in SPRR5-deficient epidermal tissue were induced in LINC00941-depleted organotypic epidermis, including many members of the human *LCE* gene family. GO term analysis of conversely regulated genes resulted in enrichment of epidermal differentiation processes, indicating that premature induction of differentiation in LINC00941-deficient epidermis appears to be caused—at least in part—by de-repression of SPRR5 (Fig 5H). To get further insight into the interrelationship between LINC00941 and SPRR5, we co-depleted both molecules in human keratinocytes at day 3 of differentiation and measured levels of several mRNAs that were inversely regulated upon single depletion of either LINC00941 or SPRR5. Interestingly,

we found that double depletion of both LINC00941 and SPRR5 led to reduced levels of keratin 1 and filaggrin (Fig EV5A and B). These data suggest that LINC00941-mediated repression of differentiation might indeed at least in part be mediated by repression of SPRR5. Taking into account that co-depletion of both LINC00941 and SPRR5 resulted in a reduction of differentiation gene expression to levels approaching the effects seen in SPRR5 depletion, one could hypothesize that SPRR5 levels need to be tightly regulated in weakly differentiated strata of the epidermis. This process appears to be controlled—at least in part—by LINC00941.

Interestingly, SPRR5 was only recently annotated as a predicted protein. Its novel gene identifier (*SPRR5*), localization downstream of the *SPRR* gene cluster as well as the general existence of repetitive proline-rich sequences suggest functional similarity of SPRR5 to

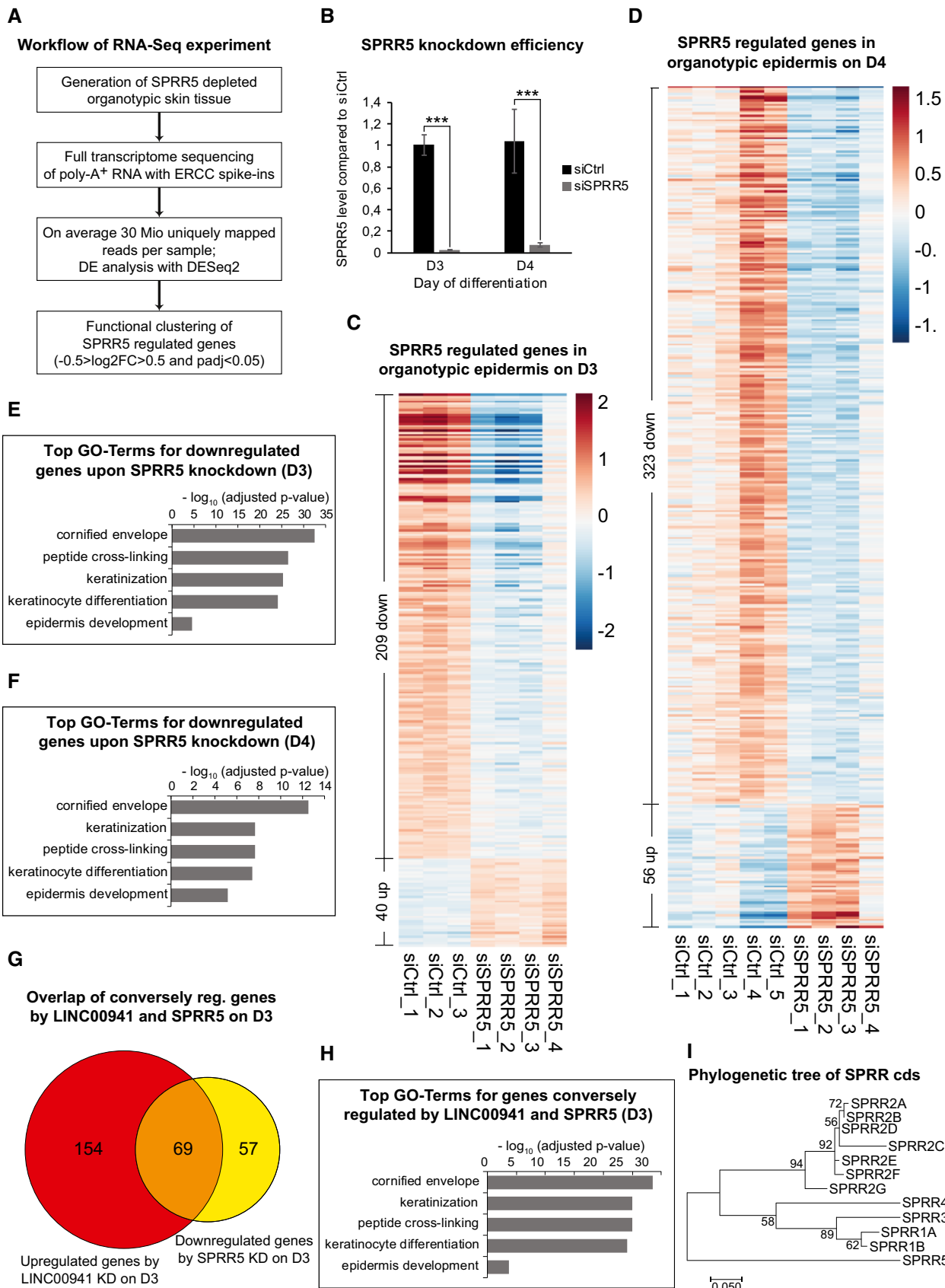


Figure 5.

Figure 5. SPRR5 controls the keratinocyte differentiation program on a global level.

- A Workflow of the performed RNA-sequencing experiment (DE = differentially expressed, $\log_2FC = \log_2(\text{fold change})$, P_{adj} = adjusted P -value).
- B Overview of SPRR5 levels in control (siCtrl) and SPRR5-deficient (siSPRR5) epidermal tissue on day 3 and day 4 as obtained by qRT-PCR analysis ($n = 3$ –5 epidermal tissue cultures/knockdown group). Data are presented as mean \pm SD. Statistical significance was tested by an unpaired t -test and corrected for multiple testing after Bonferroni (***)adj. P -value < 0.001 .
- C, D Heatmaps of differentially expressed genes ($P_{\text{adj}} < 0.05$ and $-0.5 > \log_2FC > 0.5$) upon SPRR5 depletion on day 3 (C) or day 4 (D) in organotypic epidermal tissue ($n = 3$ –5 epidermal tissue cultures/knockdown group).
- E, F GO term analysis of downregulated ($P_{\text{adj}} < 0.05$ and $-0.5 > \log_2FC$) genes in SPRR5-deficient organotypic epidermal tissue on day 3 (E) and day 4 (F) ($n = 3$ –5 epidermal tissue cultures/knockdown group).
- G Venn diagram of genes that are upregulated ($P_{\text{adj}} < 0.05$ and $\log_2FC > 1$) after LINC00941 depletion (red) and downregulated ($P_{\text{adj}} < 0.05$ and $-1 > \log_2FC$) in SPRR5-deficient (yellow) organotypic epidermal tissue on day 3 ($n = 3$ –5 epidermal tissue cultures/knockdown group).
- H GO term analysis of genes conversely (upregulated in LINC00941-deficient and downregulated in SPRR5-deficient samples) regulated by LINC00941 and SPRR5 in day 3 epidermal tissue ($n = 3$ –5 epidermal tissue cultures/knockdown group).
- I Phylogenetic analysis of all known human *SPRR* coding sequences (cds) by means of a maximum-likelihood approach. The length of the horizontal bar indicates 0.05 mutations/site. Sequence similarity suggests a common ancestor of all *SPRR*s, but a distinct composition of *SPRR*s.

other SPRR proteins which act as structural proteins involved in the formation of the cornified envelope. However, to our knowledge, depletion of none of the previously known SPRR proteins resulted in significant phenotypic abnormalities of the murine epidermal differentiation program. In contrast to this, we were able to show that SPRR5 deficiency leads to a highly impaired differentiation pattern in epidermal tissue. To approach this discrepancy between observed phenotypic effects of SPRR5 and predicted functional similarity to other SPRRs, we analyzed evolutionary relationships among all human SPRR proteins and SPRR5 generating a phylogenetic tree. Interestingly, SPRR5 did not cluster in one of the two SPRR subfamilies but lies isolated (Fig 5I). These findings suggest that phylogenetically as well as functionally, SPRR5 drastically differs from other members of the human SPRR family by operating as a crucial regulator of human epidermal differentiation. Furthermore, SPRR5 appears to act downstream of LINC00941 which exerts at least parts of its function for epidermal homeostasis by repressing SPRR5 in weakly differentiated strata of the human epidermis. Based on our observation of inverse regulation of LINC00941 and SPRR5 in epidermal homeostasis, we analyzed regulation of both molecules in basal and squamous cell carcinoma and in psoriasis using publicly available RNA-Seq datasets as described in the Method section (Dataset EV2). This analysis suggested converse regulation of LINC00941 and SPRR5, which is in agreement with the proposed suppression of SPRR5 by LINC00941 and highlights the importance of both molecules for maintaining a proper epidermal homeostasis. While the modes of action of LINC00941- and SPRR5-mediated regulation of skin homeostasis remain unclear, we observed increased nuclear enrichment of LINC00941 compared to mRNAs and identified a role in repressing premature activation of LCE and SPRR gene clusters. These findings might suggest a potential role of LINC00941 *in trans* as a transcriptional regulator of these two gene clusters, including the SPRR5 gene. Nevertheless, significant amounts of LINC00941 were also detected in the cytoplasm. While more work is needed to illuminate the mode of action of LINC00941, the data at hand show clear differences to ANCR and TINCR, two other lncRNAs involved in regulation of human epidermal homeostasis. In contrast to LINC00941, TINCR was shown to be enriched in highly differentiated strata of the epidermis and plays a role as a positive regulator of epidermal differentiation. ANCR, on the other hand, showed an enrichment in non-differentiated keratinocytes, similar to LINC00941. However, ANCR appears to play a role in maintaining the epidermal

progenitor state, likely by mediating epigenetic repression of transcription factors MAF and MAFB [8]. Based on the data shown here, LINC00941 might play an important role in weakly differentiated keratinocytes of human epidermis, likely repressing premature differentiation by modulating SPRR5 abundance. Therefore, all three lncRNAs appear to have distinct roles and modes of action in the regulation of human epidermal homeostasis.

In conclusion, these results shed light onto another aspect of the highly complex regulatory network of epidermal homeostasis, which might be crucial for comprehending epidermis development and the molecular basis of skin diseases.

Materials and Methods

Tissue culture

Pooled primary human keratinocytes from different donors were obtained from PromoCell (Lot.No.: 1020401, 1040101, and 407Z001) or Lonza (Lot.No.: 0000402834) and grown in a 1:1 mixture of KSF-M (Gibco) and Medium 154 for keratinocytes (Gibco), supplemented with Human Keratinocyte Growth Supplement, epidermal growth factor, bovine pituitary extract, and 1 \times Antibiotic-Antimycotic (all supplements from Gibco). Cells were cultured at 37°C in a humidified chamber with 5% CO₂. *In vitro* keratinocyte differentiation was induced by raising the calcium concentration in the medium to 1.2 mM and seeding cells at full confluency.

RNA knockdown

siRNA pools of 11–30 different siRNAs, combining potent on-target gene silencing with negligible off-target effects, were synthesized and obtained from siTOOLS [23]. Pan-p63 siRNAs (sense: 5'cgacagucuguacaauuu3', antisense: 5'aaaauuguacaagacugucg3') and siRNA Control (sense: 5'guagaucauuuugaagg3', antisense: 5'ccuua-caauaugaacuac3') were purchased from biomers.net and annealed in annealing buffer (30 mM HEPES, 2 mM MgAc, 100 mM KAc) by heating to 95°C for 3 min followed by 1-h incubation at 37°C. For siRNA transfer, 5–6 million primary human keratinocytes were electroporated with 1 nmol annealed siRNAs or siPools, respectively, using the Amaxa human keratinocyte Nucleofector kit (Lonza) according to the manufacturer's instructions and the program T-018

of the Amaxa Nucleofector II device. Co-depletion experiments were performed with a total of 2 nmol siRNA. After nucleofection, cells recovered for 12–24 h.

Organotypic human epidermal tissue

For the generation of organotypic human epidermal tissue, 500,000 human keratinocytes that have been nucleofected with siRNAs were seeded onto a devitalized dermal matrix and raised to the air–liquid interface to initiate stratification and differentiation, as described previously [19,24].

Immunofluorescence and tissue analysis

Seven micrometer thick cross sections of human organotypic skin cultures were fixed in either 100% acetone, ethanol, or methanol for 10 min at -20°C followed by blocking in PBS with 10% bovine calf serum (BCS) for 20 min at RT. Antibodies were diluted in PBS with 1% BCS and incubated with the sections for 1 h or overnight. Primary antibodies included the following: collagen type VII (Calbiochem, 234192 for rabbit; Merck Millipore, MAB1345 for mouse) at 1:400 (rabbit) or 1:800 (mouse) dilution, filaggrin (Santa Cruz, sc-66192) at 1:50 dilution, keratin 10 (NeoMarkers, MS-611-P) at 1:400 dilution, and loricrin (Covance, PRB-145P) at 1:800 dilution. Alexa-555-conjugated goat anti-mouse and goat anti-rabbit IgG (Molecular Probes, 1:300 dilution), and Alexa-488-conjugated goat anti-rabbit and goat anti-mouse IgG (Molecular Probes, 1:300 dilution) were used as secondary antibodies. Unbound antibodies were washed off with PBS (three times, 5 min, RT), and nuclei were stained with 4 mg/l Hoechst 33342 (Thermo Fisher Scientific, H1399) in PBS. Finally, slides were mounted in ProLong Gold Antifade Mountant (Thermo Fisher Scientific) and analyzed with an Axiovert 200M fluorescence microscope and the AxioVision Software (Carl Zeiss).

Western blot

Protein lysates from *in vitro* differentiated keratinocytes were obtained by scraping cells into a suitable amount of RIPA buffer and snap-freezing. Lysates were cleared for 15 min, full speed, 4°C , and the protein concentration was determined via Bradford assay. Thirty micrograms of total protein was separated on a 10% SDS–PAGE and transferred onto the Amersham Hybond ECL membrane by semi-dry blot. Blocking and antibody dilution was done in 5% milk in TBS-T. Primary antibodies included keratin 1 (Covance, PRB-149P) at 1:1,000 dilution, loricrin (Covance, PRB-145P) at 1:1,000 dilution, and β -actin (Abcam, ab6276) at 1:10,000 dilution. Secondary antibodies utilized were IRDye 800CW goat anti-rabbit and IRDye 680 goat anti-mouse (PN 926-32220), both at a 1:15,000 dilution. Signals were analyzed with the Odyssey Infrared Imager (LI-COR Biosciences).

qRT–PCR analysis

Total RNA from keratinocytes was isolated with TRIzol (Invitrogen) according to the manufacturer's instructions and quantified by NanoDrop. Total RNA from organotypic skin cultures was isolated using the RNeasy Plus mini kit (Qiagen) according to the

manufacturer's instructions. One microgram total RNA was subjected to reverse transcription with the iScript cDNA synthesis kit (Bio-Rad). For RNA isolated with TRIzol, genomic DNA was removed using DNase I (Thermo Fisher Scientific) prior to cDNA synthesis. For qRT–PCR measurements, SsoFast EvaGreen (Bio-Rad) or the Takyon Mix (Eurogentec) was used with the CFX96 Touch Real-Time PCR Detection System (Bio-Rad). Samples were run at least in duplicates and normalized to ribosomal protein L32 mRNA. Statistical significance was tested by an unpaired *t*-test and corrected for multiple testing after Bonferroni *et al* (*adj. *P*-value < 0.05, **adj. *P*-value < 0.01, ***adj. *P*-value < 0.001, and n.s. = not significant). For a list of primer sequences see Table 1.

Subcellular fractionation

Cell fractionation was performed as described [25] with modifications described below. All subsequent steps have been conducted on ice or at 4°C and in the presence of 50 units RiboLock RNase Inhibitor (ThermoFisher, EO0381) and Protease inhibitors cOmplete (Roche, 11873580001) according to manufacturer's instructions using RNase-free equipment. After incubation with cytoplasmic lysis buffer for 10 min on ice, it was layered onto 500 μl sucrose buffer and centrifuged at 16,000 *g* for 10 min. The supernatant corresponding to the cytoplasmic fraction was carefully removed. The nuclei pellet was gently resuspended in nuclei wash buffer and centrifuged at 1,500 *g* for 1 min. The RNA was extracted as described before.

Quantification of RNA molecules per cell

An artificial RNA control was generated with the SP6 RNA Polymerase *in vitro* transcription system (NEB, M0207) according to manufacturer's instructions and quantified by NanoDrop. The reaction was carried out at 37°C for 2 h. Residual plasmid DNA was removed using DNase I (Thermo Fisher Scientific) prior to cDNA synthesis. *In vitro* transcribed RNA was subjected to reverse transcription with the iScript cDNA synthesis kit (Bio-Rad). The cDNA products were diluted in series to generate a standard curve ranging 10^3 – 10^6 copies. qPCR data analysis was performed essentially as described before with total RNA extracted from 1 – 5×10^6 keratinocytes and recalculated to reflect single-cell analysis.

Northern blot analysis

15–25 μg total RNA from keratinocytes in different differentiation states was separated on a formaldehyde agarose gel. After blotting the RNA onto Amersham Hybond-N+ membrane and UV-crosslink at 254 nm, the membrane was prehybridized at 40 – 50°C with 1 mg herring sperm DNA (Promega) in hybridization solution (5 \times SSC, 20 mM Na_2HPO_4 , 7% SDS, 0.02% albumin fraction V, 0.02% Ficol-1400, 0.02% polyvinylpyrrolidone K30). For transcript detection, 20 pmol antisense DNA-oligos (see Table 2) was labeled in a 20 μl T4 PNK reaction (Thermo Fisher Scientific) with 20 μCi ^{32}P , purified with a G-25 column (GE Healthcare), and incubated with the prehybridized membrane overnight. After washing of the membrane (10 min each, 40 – 50°C , twice with 5 \times SSC and 1% SDS, and once with 1 \times SSC and 1% SDS), a phosphorimager screen was used to

Table 1. List of utilized qRT-PCR primers.

Name	Sequence (5'–3')
L32_F	AGGCATTGACAACAGGGTTC
L32_R	GTTGCACATCAGCAGCACTT
SPRR5_F	AGCAGCTGCAGTTCCATCT
SPRR5_R	AAACAGGAGCTGAGGGGAAG
Pan-p63_F	GACAGGAAGGCGGATGAAGATAG
Pan-p63_R	TGTTTCTGAAGTAAGTGCTGGTGC
FLG_F	AAAGAGCTGAAGGAACCTCTGG
FLG_R	AACCATATCTGGTCTATCTGG
LOR_F	CTCTGTCTGCGGCTACTCTG
LOR_R	CACGAGTCTGAGTGACCTG
KRT1_F	TGAGCTGAATCGTGTGATCC
KRT1_R	CCAGGTCAATCAGCTTGTTTC
KRT10_F	GCAAATGAGAGCTGACTG
KRT10_R	CAGTGGACACATTCGAAGG
SPRR1A_F	CAGCCATTCTGCTCCGTAT
SPRR1A_R	GGCTGGCAAGGTTGTTTCAC
SPRR2A_F	ACACAGGGAGCTTCTTTCTCC
SPRR2A_R	CCAGGACTTCTTTGCTCAGT
SPRR2D_F	TCGTTCCACAGCTCCACTTG
SPRR2D_R	CAGGCCACAGTTAAGGAGA
SPRR3_F	CCTCGACCTTCTCTGCACAG
SPRR3_R	GGTTGTTTACCTGCTGCTG
LCE1A_F	GAAGCGGACTCTGCACCTAGAA
LCE1A_R	AGGAGACAGGTGAGGAGGAAATG
LCE 1E_F	TGAAGTGGACCTTGACTTCTCTC
LCE 1E_R	CTCCAGGCAAGACTTCAAGC
LCE2A_F	TGGAGAAACTTGCAACCAGGA
LCE2A_R	CCTCACAAGGTGTGTACAGCC
LCE2D_F	GGACGTGTCTGTGCTTTTGC
LCE2D_R	CTTGGGAGGACATTTGGGAGG
LCE3A_F	TGTCTGCCTCCAGCTTCTCT
LCE3A_R	AGTTGGAGCTCTGGCAACG
LCE3D_F	TCTTGATGCATGAGTTCCAGGA
LCE3D_R	TGGACATCAGACAGGAAGTGC
LCE4A_F	CCCCCTCCCAAGTGTCTAT
LCE4A_R	GAGCCACAGCAGGAAGAGAT
LCE5A_F	CCCAGGTGCTGAAGATGTGT
LCE5A_R	ATGGAGTGAACATGGGCAGG
LCE6A_F	GTCCTGATCTCTCTCTGCTCT
LCE6A_R	CAAGATTGCTGCTTCTGCTGT
LINC00941_F	GACCTTTTCAGGCCAGCATT
LINC00941_R	ACAATCTGGATAGAGGGCTCA
Linc01527_F1	GCCTCTCTGCAAGTGTGA
Linc01527_R1	TCCTCATTTATGACATTTTCAGTCTC
Linc01527_F2	ACATGCCAGTGAAGTCTGTTCA

Table 1. (continued)

Name	Sequence (5'–3')
Linc01527_R2	AGTCATGTGAGGCAGTTCCA
Linc01527_F3	TCCCCCTACCTCTCATAGGC
Linc01527_R3	AGATGAACAGACTTCACTGGCA
C1orf68_F	TTCTGGCCCCCTCTCTGTTA
C1orf68_R	GGGACTGTACTAACTCTGGC
CALB1_F	TGGCTTTGTCGGATGGAGGG
CALB1_R	GGTTGCGGCCCAACTCTA
ELOVL3_F	TTCGAGGAGTATTGGGCAAC
ELOVL3_R	GAAGATTGCAAGGCAGAAGG
ALOX12B_F	AGACTGCAATTCGGATCAC
ALOX12B_R	TGTGGAATGCCTGGAGAAG
NEAT1_F	TTGCATAGCTGAGCGAGCCC
NEAT1_R	CTGCTGCGGCCTATTCTCTCC
GAPDH_F	GAAGAGAGAGACCCTCACTGCTG
GAPDH_R	ACTGTGAGGAGGGGAGATTCAGT
preGAPDH_F	CCAGACTGTGGGTGGCAGTG
preGAPDH_R	TGGCTGCAACTGAAGGCTCC

accumulate the radioactive signal, which was detected with the Personal Molecular Imager (Bio-Rad).

Full transcriptome RNA sequencing

Organotypic epidermal tissue was harvested on days 2, 3, or 4, and RNA was isolated using the RNeasy Plus mini kit (Qiagen), according to the manufacturer's instructions. Library preparation and mRNA sequencing were carried out according to the Illumina TruSeq Stranded mRNA Sample Preparation Guide, the Illumina HiSeq 1000 System User Guide (Illumina), and the KAPA Library Quantification Kit—Illumina/ABI Prism User Guide (Kapa Biosystems), with minor modifications. In brief, mRNA molecules were purified using oligo-dT probes immobilized on magnetic beads starting with 250 ng of total RNA supplied with ERCC spike-ins [26]. Chemical fragmentation of the mRNA to an average insert size of 200–400 bases was performed using divalent cations under elevated temperature (94°C, 4 min). First-strand cDNA was produced by reverse transcription with random primers. Actinomycin D was added to improve strand specificity by preventing spurious DNA-dependent synthesis. Blunt-ended second-strand cDNA was synthesized using DNA polymerase I, RNase H, and dUTP nucleotides. The resulting cDNA fragments were adenylated at the 3' ends, the indexing adapters were ligated, and subsequently, specific cDNA libraries were created by PCR enrichment. The libraries were quantified using the KAPA SYBR FAST ABI Prism Library Quantification Kit. Equimolar amounts of each library were used for cluster generation on the cBot (TruSeq SR Cluster Kit v3). The sequencing run was performed on a HiSeq 1000 instrument using the indexed, 1 × 50 cycles single-end protocol and TruSeq SBS v3 reagents according to the Illumina HiSeq 1000 System User Guide. Image analysis and base calling resulted in .bcl files, which were converted into .fastq files by the

Table 2. Utilized probes for northern blot analysis.

Name	Sequence (5'–3')
GAPDH #1	CATGGACTGTGGTCATGAGTCCTCCACGATACCAAAGTT
GAPDH #2	GAATTTGCCATGGGTGGAATCATATTGGAACATGTAACCATGTAGTTGAGG
Out_Exon1_SPRR5	GATGCTCTGAGCCTATCTACCTTTATATACCTCTCATCCCTGCCTGAGG
Exon1_SPRR5	CAAGGTTACCAGCGACTGGAGCAGATAGGTGTGGAGGGGTTT
Intron_SPRR5	CCCACACTACTGCTGGATAACTTGCTGGACCCAAGATAGGTTTGTAC
Exon2_SPRR5_Probe1	CACACTGCTTCTGCTTCTGCTGAGACATTCTGGGCTGGACTGCAACTGG
Exon2_SPRR5_Probe2	CAAGGCTGCTTGGTCTGTTGGGGTGGGGGGCAGTAC
Exon2_SPRR5_Probe3	GATCACATGCCAGGGCTTACTTCTGCTTGGACGTCTGGCAC
Exon2_SPRR5_ProbePool_1	TGTGGAGTGAAGATGCTGG
Exon2_SPRR5_ProbePool_2	AGAGTAGAGCTCGAGGAAGC
Exon2_SPRR5_ProbePool_3	CAGGGCAATGTAGATGCATG
Exon2_SPRR5_ProbePool_4	GCCAGGGAATTCTGTTTTA
Exon2_SPRR5_ProbePool_5	TGCTGGCCCAGAAGGAAGT
Exon2_SPRR5_ProbePool_6	TGGTGAGCAGGGCTTTGCTT
Exon2_SPRR5_ProbePool_7	TGTGGCTGCATCCAGAAGCA
Exon2_SPRR5_ProbePool_8	CCTCTCCTGCAAGTGTGAAG
Exon2_SPRR5_ProbePool_9	ACTGCAGCTGCTAATTAAGA
Exon2_SPRR5_ProbePool_10	GATCCTTGCTGAGATGGAA
Exon2_SPRR5_ProbePool_11	CATGCCGCTCATGTTCCAG
Exon2_SPRR5_ProbePool_12	GGTAGGAGAAGATGCCTGTG

CASAVA1.8.2 software. Library preparation and RNA-Seq were performed at the service facility “KFB” (Regensburg).

annotation clustering was performed using the David 6.8 database [33,34] as well as the Enrichr tool [35,36].

Bioinformatic and statistical analysis of RNA-sequencing data

- (i) *Preprocessing*: Quality of sequencing data from the RNA-Seq libraries was examined using FASTQC (<http://www.bioinformatics.babraham.ac.uk/projects/fastqc/>), and size, adapter, and quality trimming was performed using Trimmomatic (ver. 0.32 [27], ILLUMINACLIP:TruSeq_s_tranded_SE.fa:2:30:10 HEADCROP:0 TRAILING:26 LEADING:26 SLIDINGWINDOW:4:15 MINLEN:25). Trimmed reads were aligned to the Homo sapiens genome (ftp://ftp.ensembl.org/pub/release-85/fasta/homo_sapiens/dna/Homo_sapiens.GRCh38.dna.primary_assembly.fa.gz) combined with ERCC sequence information [26] using STAR [28]. The mapped reads were then assessed on the gene level using featureCounts from the Rsubread R-library [29] based on annotation information from Ensembl (GRCh38.p7 release-85). Following alignment, further quality control was performed using QoRTs [30].
- (ii) *Differential expression analysis*: Count data at the gene level were analyzed with DESeq2 [31] using ERCC spike-ins for library size normalization. All treatment comparisons were performed and corrected for multiple testing using FDR [32]. Genes that met the indicated \log_2 (fold change) restraint and a false discovery rate < 0.05 (“ P_{adj} ”) were considered significant differentially expressed.
- (iii) *Heatmap generation and functional annotation*: Heatmaps were generated with pheatmap [29] after variance stabilization transformation of count data with DeSeq2. Functional

Phylogenetic analysis of human SPRRs

The coding sequences for all human SPRR proteins were extracted from Ensembl [37], and the evolutionary history was inferred by using the maximum-likelihood method based on the Tamura–Nei model [38]. The tree with the highest log-likelihood (–761.45) is shown. The percentage of trees in which the associated taxa clustered together is shown next to the branches. Initial tree(s) for the heuristic search were obtained automatically by applying Neighbor-Join and BioNJ algorithms to a matrix of pairwise distances estimated using the maximum composite likelihood (MCL) approach and then selecting the topology with superior log-likelihood value. A discrete gamma distribution was used to model evolutionary rate differences among sites [five categories (+G, parameter = 5.2252)]. The tree is drawn to scale, with branch lengths measured in the number of substitutions per site. Codon positions included were 1st + 2nd + 3rd + non-coding. All positions containing gaps and missing data were eliminated. There were a total of 137 positions in the final dataset. Evolutionary analyses were conducted in MEGA7 [39], and 1,000 bootstrap iterations were performed.

External datasets and publicly available analysis tools

The protein-coding potential of LINC00941 (Ref_SeqID NR_040245.1) was calculated with the Coding-Potential Assessment Tool (CPAT [11], iSeeRNA [12], Lncident [13], and Coding Potential Calculator CPC2 [14]). Analysis of LINC00941 regulated genes per

chromosome was done in comparison with the Human genes (GRCh38.p10) downloaded from BioMart (Ensembl). For p63 regulation of SPRR5 in keratinocytes, published p63 ChIP-Seq datasets from Kouwenhoven *et al* [20] (GSE59827) and Bao *et al* [21] (GSE67382) keratinocytes were downloaded from the Gene Expression Omnibus (GEO) database [40] and uploaded into UCSC [41] to visualize the peak location with respect to SPRR5. Furthermore, the prediction of upstream transcription factors for SPRR5 was done with the ARCHS⁴ tool from the Ma'ayan Lab [42].

Inverse regulation of SPRR5 and LINC00941 was tested using publicly available RNA-Seq datasets from squamous cell carcinoma (GSE84293), basal cell carcinoma (GSE58375; both Smoothed inhibitor-sensitive and Smoothed inhibitor-resistant cancer types) and psoriasis (GSE83645) by mapping the reads to hg38 with Bowtie2 (version 2.3.3.1; for GSE83645) [43] or STAR (version 2.5.2b) [28] in either paired or single-stranded mode, depending on the nature of the RNA-Seq data with default settings (except for GSE58375, which was done with `-outFilterScoreMinOverLread 0,-outFilterMatchNminOverLread 0, and -outFilterMatchNmin 0`). The resulting aligned reads were counted on the gene level with HTSeq [44] (version 0.6.1.post1, `-m union, -a 10, -s no`) using a hg38 gtf file downloaded from UCSC table browser (download date 2016-02) that was supplemented with the coordinates for the SPRR5 gene. Count data were analyzed with DESeq2 [31] using standard settings, and SPRR5 or LINC00941 was considered as differentially expressed when either $-0.5 > \log_2(\text{fold change})$ or $\log_2(\text{fold change}) > 0.5$ was met.

RACE analysis

RACE (rapid amplification of cDNA ends) was performed with the FirstChoice RLM-RACE Kit (Ambion) according to the manufacturer's instructions in combination with the Expand Long Template PCR system (Roche), RNA obtained from differentiated keratinocytes, and gene-specific primers. PCR products were isolated via the NucleoSpin Gel and PCR Clean-up kit (Macherey-Nagel), cloned into pGEM-TEasy (Promega) and sequenced by Macrogen. Primer sequences were 5'outer: CTGCCAGAGGAATTCTGTTTAAATG, 5'inner: GAACCA-GATCCTGTCTGAGAT, 3'outer: CAAGTCCAGCCAGAATGTCTC, 3'inner: TCTCAGCAGAAGCAGAAGCAGT. PCR conditions were as follows:

Initial denaturation	94°C	3 min	
Amplification	94°C	30 s	25–30×
	57°C	30 s	
	68°C	90 s	
Final extension	68°C	7 min	

Data availability

The RNA-sequencing data from this publication have been deposited to the NCBI's Gene Expression Omnibus database and assigned the identifier GSE118077 (<https://www.ncbi.nlm.nih.gov/geo/query/acc.cgi?acc=GSE118077>). Itemized lists of utilized qRT-PCR primers and northern blot probes (Tables 1 and 2).

Expanded View for this article is available online.

Acknowledgements

We thank Thomas Stempfl (genomics core facility, "KFB" at the University of Regensburg) as well as Andrea Eder, Johanna Heimbucher, and Gerhard Lehmann for technical assistance and Gunter Meister, Julia Engelmann and Jörn Hendrik Reuter for discussions. Our research is supported in part by grants from the Deutsche Forschungsgemeinschaft (SFB 960 to M.K., research grant KR 3468/2-1 to M.K.) and the Beiersdorf AG.

Author contributions

CZ and JG designed and executed experiments, analyzed data, and wrote the manuscript. SF, JS, and BF executed experiments and analyzed data. NS analyzed data. RS, AB, and RM analyzed data and designed experiments. SH and MK designed experiments, analyzed data, and wrote the manuscript.

Conflict of interest

The authors declare that they have no conflict of interest.

References

- Blainpain C, Fuchs E (2009) Epidermal homeostasis: a balancing act of stem cells in the skin. *Nat Rev Mol Cell Biol* 10: 207–217
- Lopez-Pajares V, Yan K, Zarnegar BJ, Jameson KL, Khavari PA (2013) Genetic pathways in disorders of epidermal differentiation. *Trends Genet* 29: 31–40
- Kopp F, Mendell JT (2018) Functional classification and experimental dissection of long noncoding RNAs. *Cell* 172: 393–407
- Bari L, Bacsa S, Sonkoly E, Bata-Csörgő Z, Kemény L, Dobozy A, Széll M (2011) Comparison of stress-induced PRINS gene expression in normal human keratinocytes and HaCaT cells. *Arch Dermatol Res* 303: 745–752
- Kretz M, Webster DE, Flockhart RJ, Lee CS, Zehnder A, Lopez-Pajares V, Qu K, Zheng GXY, Chow J, Kim GE *et al* (2012) Suppression of progenitor differentiation requires the long noncoding RNA ANCR. *Genes Dev* 26: 338–343
- Kretz M, Sipsashvili Z, Chu C, Webster DE, Zehnder A, Qu K, Lee CS, Flockhart RJ, Groff AF, Chow J *et al* (2013) Control of somatic tissue differentiation by the long non-coding RNA TINCR. *Nature* 493: 231–235
- Lee CS, Mah A, Aros CJ, Lopez-Pajares V, Bhaduri A, Webster DE, Kretz M, Khavari PA (2018) Cancer-associated long noncoding RNA SMRT-2 controls epidermal differentiation. *J Invest Dermatol* 138: 1445–1449
- Lopez-Pajares V, Qu K, Zhang J, Webster DE, Barajas BC, Sipsashvili Z, Zarnegar BJ, Boxer LD, Rios EJ, Tao S *et al* (2015) A LncRNA-MAF:MAFB transcription factor network regulates epidermal differentiation. *Dev Cell* 32: 693–706
- Sonkoly E (2005) Identification and characterization of a novel, psoriasis susceptibility-related noncoding RNA gene, PRINS. *J Biol Chem* 280: 24159–24167
- Yan X, Zhang D, Wu W, Wu S, Qian J, Hao Y, Yan F, Zhu P, Wu J, Huang G *et al* (2017) Mesenchymal stem cells promote hepatocarcinogenesis via lncRNA-MUF interaction with ANXA2 and miR-34a. *Cancer Res* 77: 6704–6716
- Wang L, Park HJ, Dasari S, Wang S, Kocher J-P, Li W (2013) CPAT: coding-potential assessment tool using an alignment-free logistic regression model. *Nucleic Acids Res* 41: e74

12. Sun K, Chen X, Jiang P, Song X, Wang H, Sun H (2013) iSeeRNA: identification of long intergenic non-coding RNA transcripts from transcriptome sequencing data. *BMC Genom* 14: S7
13. Han S, Liang Y, Li Y, Du W (2016) Lncident: a tool for rapid identification of long noncoding RNAs utilizing sequence intrinsic composition and open reading frame information. *Int J Genomics* 2016: 9185496
14. Kang Y-J, Yang D-C, Kong L, Hou M, Meng Y-Q, Wei L, Gao G (2017) CPC2: a fast and accurate coding potential calculator based on sequence intrinsic features. *Nucleic Acids Res* 45: W12–W16
15. Kyriotou M, Huber M, Hohl D (2012) The human epidermal differentiation complex: cornified envelope precursors, S100 proteins and the ‘fused genes’ family: human epidermal differentiation complex. *Exp Dermatol* 21: 643–649
16. Mischke D, Korge BP, Marenholz I, Volz A, Ziegler A (1996) Genes encoding structural proteins of epidermal cornification and S100 calcium-binding proteins form a gene complex (‘epidermal differentiation complex’) on human chromosome 1q21. *J Invest Dermatol* 106: 989–992
17. Mills AA, Zheng B, Wang X-J, Vogel H, Roop DR, Bradley A (1999) p63 is a p53 homologue required for limb and epidermal morphogenesis. *Nature* 398: 708–713
18. Romano R-A, Smalley K, Magraw C, Serna VA, Kurita T, Raghavan S, Sinha S (2012) ΔNp63 knockout mice reveal its indispensable role as a master regulator of epithelial development and differentiation. *Development* 139: 772–782
19. Truong AB, Kretz M, Ridky TW, Kimmel R, Khavari PA (2006) p63 regulates proliferation and differentiation of developmentally mature keratinocytes. *Genes Dev* 20: 3185–3197
20. Kouwenhoven EN, Oti M, Niehues H, van Heeringen SJ, Schalkwijk J, Stunnenberg HG, van Bokhoven H, Zhou H (2015) Transcription factor p63 bookmarks and regulates dynamic enhancers during epidermal differentiation. *EMBO Rep* 16: 863–878
21. Bao X, Rubin AJ, Qu K, Zhang J, Giresi PG, Chang HY, Khavari PA (2015) A novel ATAC-seq approach reveals lineage-specific reinforcement of the open chromatin landscape via cooperation between BAF and p63. *Genome Biol* 16: 284
22. Cavazza A, Miccio A, Romano O, Petiti L, Malagoli Tagliazucchi G, Peano C, Severgnini M, Rizzi E, De Bellis G, Bicciato S et al (2016) Dynamic transcriptional and epigenetic regulation of human epidermal keratinocyte differentiation. *Stem Cell Reports* 6: 618–632
23. Hannus M, Beitzinger M, Engelmann JC, Weickert M-T, Spang R, Hannus S, Meister G (2014) siPools: highly complex but accurately defined siRNA pools eliminate off-target effects. *Nucleic Acids Res* 42: 8049–8061
24. Sen GL, Reuter JA, Webster DE, Zhu L, Khavari PA (2010) DNMT1 maintains progenitor function in self-renewing somatic tissue. *Nature* 463: 563–567
25. Mayer A, di Iulio J, Maleri S, Eser U, Vierstra J, Reynolds A, Sandstrom R, Stamatoyannopoulos JA, Churchman LS (2015) Native elongating transcript sequencing reveals human transcriptional activity at nucleotide resolution. *Cell* 161: 541–554
26. External RNA Controls Consortium (2005) Proposed methods for testing and selecting the ERCC external RNA controls. *BMC Genom* 6: 150
27. Bolger AM, Lohse M, Usadel B (2014) Trimmomatic: a flexible trimmer for Illumina sequence data. *Bioinformatics* 30: 2114–2120
28. Dobin A, Davis CA, Schlesinger F, Drenkow J, Zaleski C, Jha S, Batut P, Chaisson M, Gingeras TR (2013) STAR: ultrafast universal RNA-seq aligner. *Bioinformatics* 29: 15–21
29. Kolde R (2012) Pheatmap: pretty heatmaps. R Package Version 61
30. Hartley SW, Mullikin JC (2015) QoRTs: a comprehensive toolset for quality control and data processing of RNA-Seq experiments. *BMC Bioinformatics* 16: 224
31. Love MI, Huber W, Anders S (2014) Moderated estimation of fold change and dispersion for RNA-seq data with DESeq2. *Genome Biol* 15: 550
32. Benjamini Y, Hochberg Y (1995) Controlling the false discovery rate: a practical and powerful approach to multiple testing. *J R Stat Soc Series B Methodol* 57: 289–300
33. Huang DW, Sherman BT, Lempicki RA (2009) Systematic and integrative analysis of large gene lists using DAVID bioinformatics resources. *Nat Protoc* 4: 44–57
34. Huang DW, Sherman BT, Lempicki RA (2009) Bioinformatics enrichment tools: paths toward the comprehensive functional analysis of large gene lists. *Nucleic Acids Res* 37: 1–13
35. Chen EY, Tan CM, Kou Y, Duan Q, Wang Z, Meirelles G, Clark NR, Ma’ayan A (2013) Enrichr: interactive and collaborative HTML5 gene list enrichment analysis tool. *BMC Bioinformatics* 14: 128
36. Kuleshov MV, Jones MR, Rouillard AD, Fernandez NF, Duan Q, Wang Z, Koplev S, Jenkins SL, Jagodnik KM, Lachmann A et al (2016) Enrichr: a comprehensive gene set enrichment analysis web server 2016 update. *Nucleic Acids Res* 44: W90–W97
37. Zerbino DR, Achuthan P, Akanni W, Amode MR, Barrell D, Bhai J, Billis K, Cummins C, Gall A, Girón CG et al (2018) Ensembl 2018. *Nucleic Acids Res* 46: D754–D761
38. Tamura K, Nei M (1993) Estimation of the number of nucleotide substitutions in the control region of mitochondrial DNA in humans and chimpanzees. *Mol Biol Evol* 10: 512–526
39. Kumar S, Stecher G, Tamura K (2016) MEGA7: molecular evolutionary genetics analysis version 7.0 for bigger datasets. *Mol Biol Evol* 33: 1870–1874
40. Barrett T, Wilhite SE, Ledoux P, Evangelista C, Kim IF, Tomashevsky M, Marshall KA, Phillippy KH, Sherman PM, Holko M et al (2013) NCBI GEO: archive for functional genomics data sets—update. *Nucleic Acids Res* 41: D991–D995
41. Kent WJ, Sugnet CW, Furey TS, Roskin KM, Pringle TH, Zahler AM, Haussler D (2002) The human genome browser at UCSC. *Genome Res* 12: 996–1006
42. Lachmann A, Torre D, Keenan AB, Jagodnik KM, Lee HJ, Silverstein MC, Wang L, Ma’ayan A (2018) Massive mining of publicly available RNA-seq data from human and mouse. *Nat Commun* 9: 1366
43. Langmead B, Salzberg SL (2012) Fast gapped-read alignment with Bowtie 2. *Nat Methods* 9: 357–359
44. Anders S, Pyl PT, Huber W (2015) HTSeq—a Python framework to work with high-throughput sequencing data. *Bioinformatics* 31: 166–169